Atomization and Sprays, vol. 7, pp. 383–406, 1997

LIGAMENT-CONTROLLED EFFERVESCENT ATOMIZATION

J. J. Sutherland, P. E. Sojka, and M. W. Plesniak
Thermal Sciences and Propulsion Center, School of Mechanical Engineering, Purdue University, West Lafayette, Indiana, USA

The operating principles and performance of a new type of spray nozzle are presented. This nozzle, termed a ligament-controlled effervescent atomizer, was developed to allow consumer product manufacturers to replace volatile organic compound (VOC) solvents with water and hydrocarbon (HC) propellants with air, while meeting the following restrictions: that the spray mean drop size remain below 70 μm, that the atomizing air consumption be less than 0.009, and that atomizer performance be uncompromised by the increase in surface tension or by changes in viscosity. The current atomizer differs from previous effervescent designs through inclusion of a porous disk located immediately upstream of the nozzle exit orifice. The purpose of this disk is to control the diameter of ligaments formed at the injector exit plane. Atomizer performance is reported in terms of the spray Sauter mean diameter, with drop size data analyzed using a model developed from first principles. The model describes the spray formation process as the breakup of individual cylindrical ligaments subject to a gas stream. Ligament breakup length is obtained using the expression of Sterling and Sleicher [1]. Ligament diameter is estimated from manufacturer-supplied pore size data for the porous disk. The model correctly predicts the experimentally observed relationship between Sauter mean diameter and air-to-liquid ratio by mass, liquid surface tension, and liquid viscosity.

INTRODUCTION

The Pollution Prevention Act of 1990 states that, if possible, pollution should be prevented at the source. This is often difficult to achieve because of the potential for transferring emissions from one medium to another. The optimum approach would be to eliminate the sources of pollution, which for some consumer product aerosol sprays are volatile organic compound (VOC) solvents and hydrocarbon (HC) propellants. Simply removing VOCs and HCs affects the quality of the spray delivered by current twin-fluid and pressure-swirl atomizers. Consequently, an atomizer whose performance is independent of solvent and propellant type would be very useful. The best situation would be an atomizer that would allow water to be substituted for the VOC solvent, air to be substituted for the HC propellant, and whose performance would remain uncompromised. This goal provides the motivation for this study.

Achieving this goal for twin-fluid atomization requires a substantial reduction in propellant consumption for three reasons. First, deceptive-packaging guidelines suggest

The authors gratefully acknowledge the support of the U.S. Environmental Protection Agency through Cooperative Agreement CR822618 with the Air and Energy Environmental Research Laboratory. Kelly Leovic was the technical monitor.

NOMENCLATURE

a	ligament radius, m	ρ	density, kg/m^3
A	area, m^2	ξ	instability wavenumber, dimensionless
ALR	air/liquid ratio by mass, dimensionless	ξ_{opt}	critical dimensionless wavenumber
d	diameter, m	σ	surface tension, kg/s^2
$\dot{m}$	mass flow rate, kg/s		
M_o	momentum rate, N		**Subscript/Superscript**
sr	slip ratio, dimensionless		
SMD	Sauter mean diameter, μm	g	atomizing gas
U	relative velocity, m/s	l	liquid
α	void fraction, dimensionless	L	ligament
β	dimensionless growth rate	0	at the nozzle exit
λ_{opt}	Weber's optimum breakup wavelength, mm	^	air
μ	viscosity, kg/m-s	E	exit

that at least 60% of a spray container be filled with product. Second, U.S. Department of Transportation container charging restrictions limit package pressures to less than 1 MPa (147 psig) for systems employing nonliquefied propellants. Finally, a minimum propellant pressure is required to supply the last of the product, so not all of the propellant mass can be used to form sprays. The result is an upper bound on atomizing air consumption of less than 0.01 of the liquid product to be dispensed.

An air–liquid ratio (ALR) by mass of 0.01 or less is outside the range of conventional twin-fluid nozzles. The only design that comes close to meeting this criterion is the effervescent atomizer. As will be demonstrated below, a new type of effervescent atomizer can achieve the goals stated above.

Effervescent atomization is characterized by actively introducing gas bubbles into a liquid flow immediately upstream of the exit orifice, thereby forming a two-phase flow. This allows an efficient transfer of energy between the atomizing gas and the liquid so a high-quality spray may be produced at ALRs lower than those required by most conventional twin-fluid atomizers.

A number of investigators have studied effervescent atomizer-produced sprays. Early work includes that of Lefebvre et al. [2], who demonstrated very good atomization with mean drop sizes comparable to those obtained with air-assist atomizers operating at much higher ALRs; that of Wang et al. [3], who showed that orifice diameter and gas injector geometry had little effect on the quality of atomization; that of Roesler and Lefebvre [4], whose photographic results showed that bubble explosions were an important mechanism in the atomization process at low ALRs and that bubble spacing influenced droplet size at these conditions; and that of Whitlow and Lefebvre [5], whose most significant result was the observation that acceptable atomization could be achieved when using an orifice geometry that turns the two-phase flow through an angle just prior to ejection from the nozzle.

Other investigators have been concerned with the influence of fluid rheology on atomizer performance. Most notable are the studies of Buckner and Sojka [6], who investigated the effects of viscosity and non-Newtonian fluid rheology on mean drop size and concluded that viscoelasticity controls spray formation, and of Geckler and Sojka [7], who developed an analytical model that successfully predicted the influence of viscoelasticity on mean drop size.

Studies most pertinent to the current work are those of Santangelo and Sojka [8] and Lund et al. [9], all of whom performed investigations of the near-nozzle breakup regions of effervescent sprays. Santangelo and Sojka [8] employed a focused-image holography system, while Lund et al. [9] used high-speed photography to obtain images of this region.

Santangelo and Sojka [8] constructed holograms for sprays formed from fluids having three different viscosities and two different surface tensions in order to study how fluid physical properties affect the near-nozzle structure and, ultimately, Sauter mean diameter (SMD). Their holograms revealed that the jump in SMD associated with operation at low air/liquid ratios was the result of a transition in near-nozzle structure from liquid breakup dominated by single bubble explosions to formation of an annular ring of smaller-diameter ligaments. Breakup of these smaller ligaments resulted in a decrease in SMD.

Lund et al. [9] utilized near-nozzle images of the breakup structure in the development of an analytical model to predict SMD. Their model is based on the ligament breakup analysis of Weber [10], whose analytical expression for the hydrodynamic instability mode having the maximum growth rate is

$$\lambda_{\text{opt}} = \sqrt{2}\pi d_L \sqrt{1 + \frac{3\mu_l}{\sqrt{\rho_l \sigma_l d_L}}} \tag{1}$$

Lund et al. [9] assumed that each ligament forms a single spherical drop with a diameter equal to the Sauter mean diameter. Initial conditions for their model were determined using the velocity slip ratio expression of Ishii [11],

$$sr = \sqrt{\frac{\rho_l}{\rho_g}} \sqrt{\frac{\sqrt{\alpha}}{1 + 75(1 - \alpha)}} \tag{2}$$

and conservation of mass for the air and liquid streams,

$$\alpha = \frac{1}{1 + \dfrac{\rho_g{}^{sr}}{\rho_l{}^{\text{ALR}}}} \tag{3}$$

After some manipulation, Lund et al. [9] showed that

$$\text{SMD} = 3\sqrt{\frac{3}{2}\sqrt{2}\pi d_L^3 \sqrt{1 + \frac{3\mu_l}{\sqrt{\rho_l \sigma_l d_L}}}} \tag{4}$$

where d_L is the ligament diameter, μ_l, ρ_l, and σ_l are the liquid viscosity, density, and surface tension, respectively, sr is the velocity slip ratio (quotient of gas and liquid velocities), ρ_g is the gas density, α is the void fraction (quotient of gas to gas-plus-liquid volumes), and λ_{opt} is Weber's [10] ligament breakup length. This model accurately predicts the viscosity and surface tension scaling observed in their experimental data.

The experimental work of Lund et al. [9] demonstrated that a sub-70 μm mean drop size spray was attainable only at air/liquid ratios above 0.02. The work of Santangelo and Sojka [8] attributed this minimum ALR to a transition in near-nozzle breakup occurring at about this air/liquid ratio. Therefore, further reduction in SMD at low air/liquid ratios is not possible without a change in the breakup structure at the exit. Ligament-controlled effervescent atomizers were designed to avoid the transition in breakup structure that occurs, allowing their use in applications that require low air consumption, i.e., consumer product sprays.

As further evidence of the potential for consumer-product spray formation via ligament-controlled effervescent atomization, the work of Whitlow and Lefebvre [5], in conjunction with that of Roesler and Lefebvre [4], Lefebvre et al. [2], and Wang et al. [3], demonstrates that effervescent atomizers are capable of achieving large cone angles with little sensitivity to exit orifice diameter. These findings indicate that a single design can be employed for a wide variety of products, thereby reducing unit costs. Collectively, this information demonstrates that ligament-controlled effervescent atomizers represent a viable alternative to current twin-fluid atomizer designs used in consumer product applications. The performance of such a device is described in the following sections.

EXPERIMENTAL APPARATUS

The atomizer, air and liquid supply systems, rheology instrumentation, drop size instrumentation, and imaging systems used to acquire the data presented here are described in the following paragraphs.

Figure 1 illustrates the ligament-controlled effervescent atomizer used in this study. It is made entirely from brass and consists of a top plate, a containment tube, an aerator tube, and an exit orifice plate. Liquid is fed into the side and flows downward through an annular gap between the containment and aerator tubes. Air, supplied from the control panel, is injected into the liquid through two holes located at the end of the aerator tube, creating a two-phase flow. The flow then passes through a porous medium before leaving through the exit orifice.

The aerator tube is 133 mm (5.25 in.) long, has an outside diameter of 3.2 mm (0.125 in.), and passes through a Caion Ultra-torr vacuum fitting, threaded into the atomizer top plate, which allows for fine adjustment of the aerator tube position relative to the exit orifice. The containment tube has an outside diameter of 50.8 mm (2 in.) and an inside diameter of 3.7 mm (0.146 in.). The gap between the aerator and containment tubes was sized at 0.3 mm (0.012 in.) in order to create a downward liquid velocity sufficient to counteract the buoyancy of the air bubbles. The exit orifice plate has a diameter of 50.8 mm (2 in.) and a thickness of 3.2 mm (0.125 in.). A 4.1 mm (0.161 in.) diameter blind hole with a depth of 2.95 mm (0.116 in.) is used to hold the porous medium in place, just upstream of the exit orifice. The exit orifice diameter is 0.38 mm (0.015 in.), and its length is 0.25 mm (0.010 in.). A very short exit length was used in order to minimize coalescence of either bubbles generated inside the atomizer or of liquid ligaments formed in the porous medium.

The porous medium was obtained from Porex Technologies. It is a polyvinylidene fluoride (PVDF) disk having a diameter of 4.1 mm (0.161 in.) and a thickness of 1.0 mm (0.039 in.). The pore diameter and porosity (a ratio of the volume of the void space to the total volume of the medium) will be shown to be important inputs to our spray formation

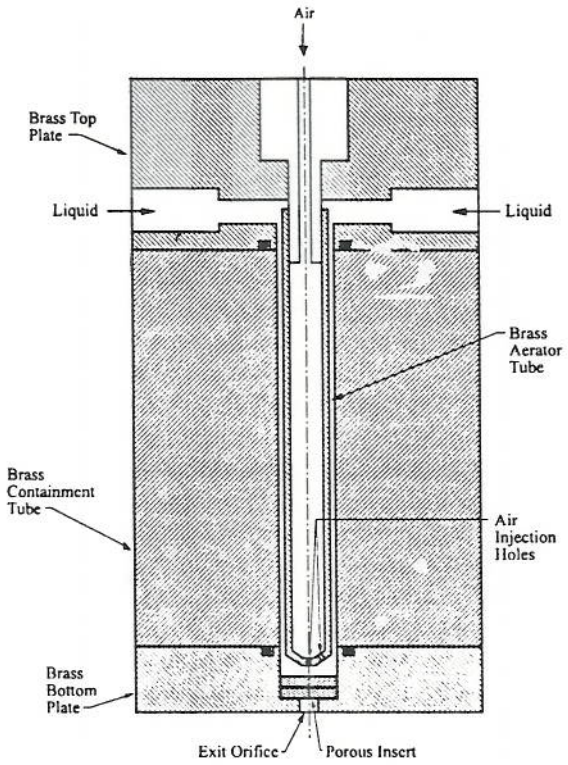

Fig. 1 Schematic of ligament-controlled effervescent atomizer.

model. Values were measured by the manufacturer using mercury-intrusion porosimetry and reported to be 37 μm and 49%, respectively [12].

High-pressure air was used as the atomizing gas and to pressurize the free surface of the liquid. The air flow rate was monitored using a Matheson 602 rotameter with a stainless steel float and regulated using a Nupro B-SS2-D needle metering valve. A Nupro C-series check valve was placed immediately upstream of the aerator tube to prevent back flow of liquid into the air supply system. Rotameter calibration was performed by collecting, timing, and measuring the volume of gas passing through the rotameter at several different rotameter settings. A straight line was fitted to the data, with a coefficient of determination (r^2) of 0.991.

The liquid was supplied from a steel sphere whose free surface was pressurized. The liquid mass flow rates for the low-viscosity fluids were monitored using a Matheson 604 rotameter with a stainless steel float, while flow rates for the higher-viscosity fluids were measured using a Matheson 605 rotameter with a stainless steel float. Flow rates were regulated using a Whitey SS-1RS4 integral needle valve. A Nupro 15 μm in-line filter was placed immediately upstream of the atomizer liquid inlet port in order to prevent clogging of the atomizer. The liquid rotameter was calibrated by collecting, timing, and measuring the volume of fluid passing through the rotameter at several different settings. Straight lines were fitted to the data for all liquids, resulting in coefficients of determination (r^2) greater than 0.95 for all cases.

The nozzle was suspended over an exhaust system for all experiments. The exhaust system contained a sump to remove liquid that collected in the bottom of the duct, and a blower to exhaust the spray and remove any airborne particles.

Since a major objective of this study was to develop an atomizer whose performance was not compromised by the viscosity and surface tension of the fluid being sprayed, accurate methods for measuring these properties were necessary. Fluid viscosity was measured using a Haake falling-ball viscometer. Viscometer accuracy was confirmed using calibration oils of 9 and 98 mPa-s with values measured to within 5% of published data. Surface tensions were measured using a CSC model 70535 du-Nuoy ring tensiometer. This instrument was calibrated by placing a known weight on the ring and measuring the resulting force. Fluid densities were calculated from the quotient of a known volume of fluid and its measured weight. Weights were measured using a Mettler model P1200N electronic balance with volumes measured using a graduated cylinder.

Drop size distribution data were obtained using a Malvern 2600 particle size analyzer fitted with a 300 mm-focal-length receiving lens. All drop size measurements were taken with the laser beam passing through the center of the spray at a location 15 cm downstream of the exit orifice. Each measurement consists of 3000 samples. A minimum of five measurements were obtained at each operating condition.

Qualitative information about breakup mechanisms leading to drop formation was obtained using high-speed photography and focused-image holography. Magnified images of near-nozzle spray structures were obtained via high-speed black-and-white photography. Images of approximately 10× magnification were obtained using a conventional Nikon 35 mm SLR camera, a 55 mm-focal length lens, and a bellows extension. The light source was a 500 ns-duration pulse generated using an EG&G Microflash. The camera was set to an *f*-stop of 1.8, with the exposure time fixed by the flash duration. Images were captured on Kodak TMAX ISO 400 black-and-white film.

Holographic images of the near-nozzle structure were obtained using the focused-image holographic system of Santangelo and Sojka [13]. A general overview of focused-image holography as a spray diagnostic tool is provided by these authors [14]. The recording medium was Agfa HD 8E75 NAH holographic plates. The holographic plate developing system used was supplied by H. I. Bjelkhagen of Northwestern University and E. Wesley of Lake Forest College. Specific details are provided by Santangelo [15].

RESULTS

Experimental results describing the performance of ligament-controlled effervescent atomizers operating at low air/liquid ratios are presented and discussed in this section. Performance was determined for a number of operating conditions and spray fluids. The parameters that were varied, and the ranges over which data were collected, are shown in Table 1.

The influences of fluid physical properties and operating conditions on SMD are considered. All drop size measurements were obtained using a Malvern particle size analyzer, with the probe volume passing through the center of the spray at a position 15 cm downstream of the exit orifice. High-speed photographs and a summary of three-dimensional holographic images of the near-nozzle breakup structure of the spray are also presented. These were instrumental in the development of a model to predict drop sizes for ligament-controlled effervescent sprays.

Table 1 Parameters for Experimental Investigation

Parameter	Range studied	Units
Viscosity (μ)	0.001–0.080	kg/m-s
Surface tension (σ)	0.030–0.067	kg/s^2
Air/liquid ratio by mass (ALR)	0.005–0.04	Dimensionless
Liquid mass flow rate ($\dot{m}_l$)	0.5–1.0	g/s

Seven different fluids representing three common viscosities and two common surface tensions were sprayed during this investigation. The physical properties of these fluids are shown in Table 2. Tap water was used for the water spray experiments. The glycerine–water mixtures are identified by their volumetric composition. The SNO oils are Texaco Solvent Neutral Oils (SNOs). Benzoil is a universal calibration oil with a surface tension similar to that of the SNO oils, but with a much lower viscosity. The oil mixtures are also identified by their volumetric composition.

The viscosities and surface tensions were chosen to span the range of current consumer products and their projected water-based counterparts. The lower value of surface tension, 0.030 kg/s^2, is characteristic of consumer products currently employing alcohol (or other VOC) carriers. The higher value, 0.067 kg/s^2, represents a water-based formulation.

The operating conditions expected to affect nozzle performance are air/liquid ratio and liquid mass flow rate. The air/liquid ratio was varied from 0.005 to 0.01. Liquid mass flow rate was varied from 0.5 to 1.0 g/s.

Figure 2 contains drop size data for the three fluids with a common surface tension (0.030 kg/s^2) that is representative of current VOC solvent-based consumer products. This figure illustrates the influence of ALR on SMD—an increase in ALR above 0.0075 reduces SMD slightly, while a reduction in ALR below 0.0075 results in a dramatic increase in mean drop size. Error bars representing 1 standard deviation are included. The data demonstrate that SMDs of less than 70 μm (within experimental uncertainty) are obtained for ALRs as low as 0.0075.

Figure 3 contains drop size data for the three fluids with a common surface tension (0.067 kg/s^2) that is representative of water-based consumer products. Again, error bars representing 1 standard deviation are included. The data demonstrate that SMDs are less than 70 μm (within experimental uncertainty) for ALRs as low as 0.0075. As with the lower-surface-tension fluids, a marked increase in SMD is observed at ALRs below 0.0075.

Table 2 Physical Properties of the Spray Fluids at Room Conditions

Fluid	Viscosity (kg/m-s)	Surface tension (kg/s^2)	Density (kg/m^3)
Water	0.001	0.072	998
63/37 Glycerine/water	0.020	0.067	1170
72/28 Glycerine/water	0.040	0.067	1197
80/20 Glycerine/water	0.080	0.067	1217
75/35 SNO 100/benzoil	0.020	0.030	840
90/10 SNO 100/SNO 320	0.040	0.030	847
30/70 SNO 100/SNO 320	0.080	0.030	855

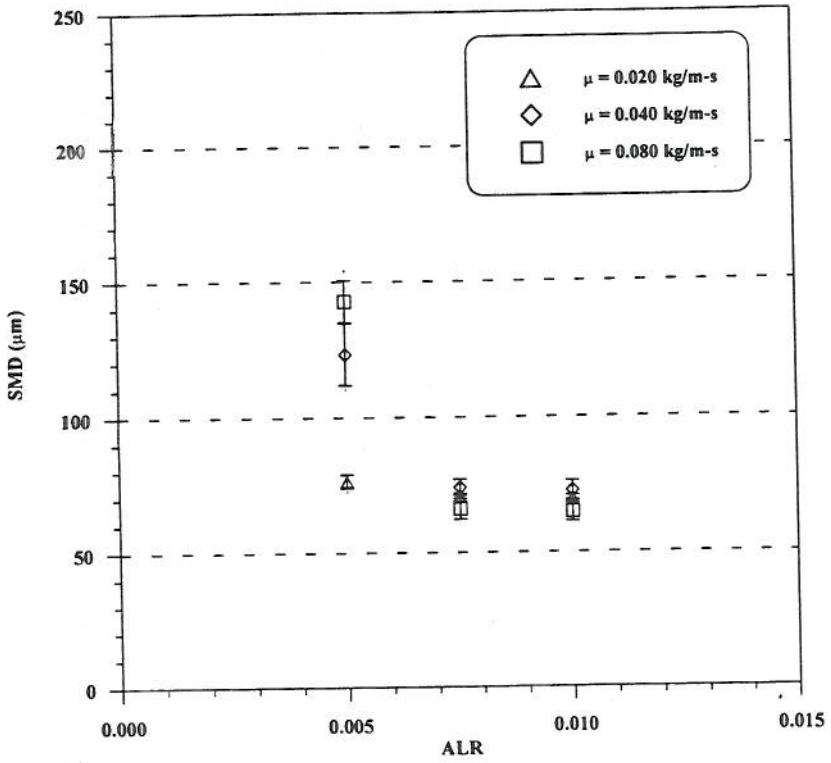

Fig. 2 Mean drop size (SMD) versus air/liquid ratio (ALR) for three fluids having viscosities of 0.020, 0.040, and 0.080 kg/m-s and a common surface tension of 0.030 kg/s^2. Error bars represent 1 standard deviation.

This behavior will be discussed when the high-speed photographs of the near-nozzle breakup structure are presented.

Figure 4 illustrates the influence of liquid mass flow rate on SMD. Data were obtained by spraying two fluids with a common viscosity (0.020 kg/m-s), but different surface tensions (0.030 and 0.067 kg/s^2) at two different mass flow rates (0.6 and 0.8 g/s). Figure 4 also demonstrates that no clear conclusions can be drawn concerning the effect of liquid mass flow rate on SMD. For the fluid having a surface tension of 0.067 kg/s^2, an increase in liquid mass flow rate resulted in a slight (<10%) decrease in SMD. However, an increase in liquid mass flow rate for a fluid having a surface tension of 0.020 kg/s^2 resulted in an increase in SMD of approximately 20%.

The most important conclusion to be drawn from Fig. 4 is that sub-70 μm mean drop size sprays were achieved at air/liquid ratios less than 0.01 for all fluids tested. This achieves the stated goals of this study. In addition, increasing the air/liquid ratio above 0.01 has little benefit toward reducing mean drop size.

Figures 2 and 3 may also be used to demonstrate the influence of fluid physical properties on SMD. Both figures indicate that the performance of ligament-controlled effervescent atomizers is relatively insensitive to the viscosity of the liquid being sprayed: Any pair of SMDs lies within the sum of their standard deviations. This is an improvement

over the small, although still noticeable, increase in mean drop size with an increase in viscosity reported by Lund et al. [9].

Comparison of the data presented in Fig. 2 with those of Fig. 3 reveals little scaling of mean drop size with surface tension; a slight increase (<10%) in mean drop size was observed upon changing the surface tension from 0.030 to 0.067 kg/s^2. This is opposite to the trend observed by Lund et al. [9], who noted a decrease in mean drop size when surface tension increased by the same amount.

Since U.S. Department of Transportation container charging restrictions limit consumer-product package pressures to less than 1 MPa, it is important to determine the supply pressures required to achieve the mean drop sizes presented in Figs. 2 through 4. This information is provided in Figs. 5 through 7, where the influence of ALR, fluid physical properties, and liquid mass flow rate are considered.

Supply pressures required when spraying fluids having a surface tension of 0.030 kg/s^2 are presented in Fig. 5. For the 0.6 g/s liquid flow rate data presented here, 440 kPa is required for the 0.020 kg/m-s liquid, 610 kPa for the 0.040 kg/m-s liquid, and 650 kPa for the 0.080 kg/m-s liquid. Supply pressures required when spraying fluids having a surface tension of 0.067 kg/s^2 are presented in Fig. 6. For the 0.6 g/s liquid flow rate data

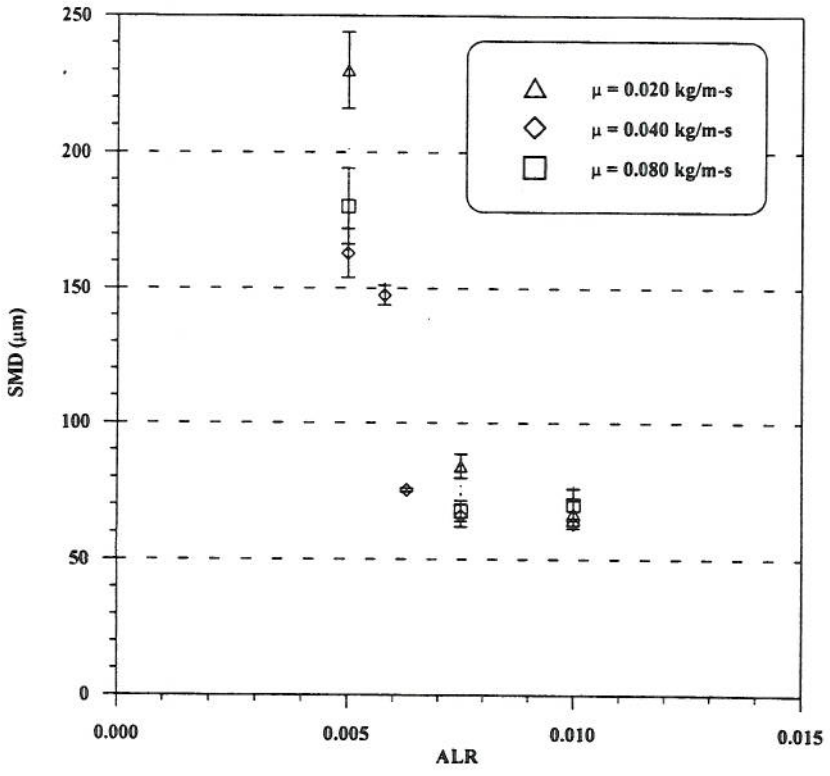

Fig. 3 Mean drop size (SMD) versus air/liquid ratio (ALR) for three fluids having viscosities of 0.020, 0.040, and 0.080 kg/m-s and a common surface tension of 0.067 kg/s^2. Error bars represent 1 standard deviation.

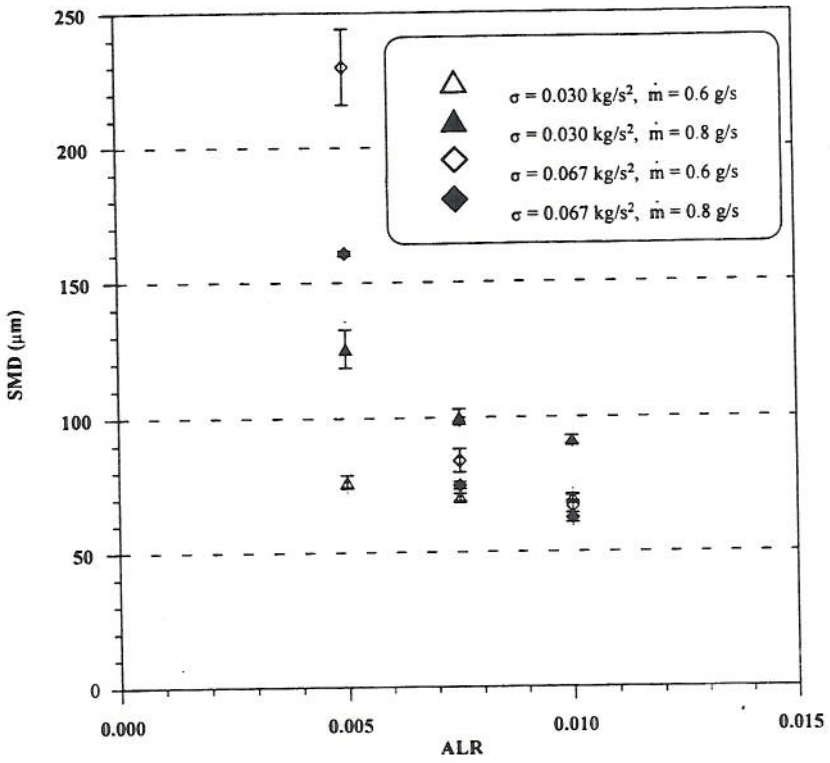

Fig. 4 Mean drop size (SMD) versus air/liquid ratio (ALR) for two fluids having surface tensions of 0.030 and 0.067 kg/s², a common viscosity of 0.020 kg/m-s, and operating at two liquid mass flow rates. Error bars represent 1 standard deviation.

presented here, only 290 kPa is required for the 0.020 kg/m-s liquid, while the 0.040 and 0.080 kg/m-s liquids require 630 and 780 kPa, respectively. (These values compare favorably with the 240 to 515 kPa supply pressures used by Lund et al. [9] in their study.) Note that in both cases, the supply pressures are well below the 1 MPa limit. Furthermore, data in both figures demonstrate that ALR has little effect on supply pressure over the range of fluid properties, mass flow rates, and ALRs considered during this study.

Figures 5 and 6 also show that a change in liquid surface tension has a mixed effect on supply pressure. Increasing the surface tension in the low-viscosity case (0.020 kg/m-s) reduces the supply pressure. Increasing the surface tension in the high-viscosity case (0.080 kg/m-s) increases the supply pressure. Increasing the surface tension in the intermediate-viscosity case (0.040 kg/m-s) has little effect on supply pressure. There is no known explanation for this behavior.

Finally, the data of Figs. 5 and 6 illustrate the expected increase in supply pressure with an increase in liquid viscosity. This relationship is characteristic of flow through porous media.

The data in Figs. 5 and 6 were obtained at a common liquid mass flow rate of 0.6 g/s. Figure 7 illustrates the influence of liquid mass flow rate on supply pressure. The data

exhibit the expected increase in supply pressure with mass flow rate, a phenomenon common to flow through porous media.

A physical explanation for the observed mean drop size behavior is provided in Figs. 8 through 12. These figures were obtained using the high-speed photographic apparatus discussed earlier.

Figures 8 and 9 compare sprays produced using the Lund et al. [9] atomizer to those produced using the ligament-controlled effervescent atomizer. The spray shown in Fig. 8 was produced using the Lund et al. [9] atomizer spraying water at a rate of 1.0 g/s with an ALR of 0.015. Figure 9 shows a spray produced using a ligament-controlled effervescent atomizer operating under the same conditions. It is obvious from the photographs that the inclusion of a porous disk results in better spray quality at low air/liquid ratios; when compared to the Lund et al. [9] nozzle, the ligament-controlled effervescent atomizer produces a larger number of smaller-diameter ligaments. It is this decrease in ligament diameter that leads directly to the decreased drop size obtained when using the ligament-controlled effervescent atomizer.

Figures 10 through 12 illustrate how the ligament formation and breakup processes vary as ALR is reduced from 0.01 to 0.005. It is clear that the number of ligaments is

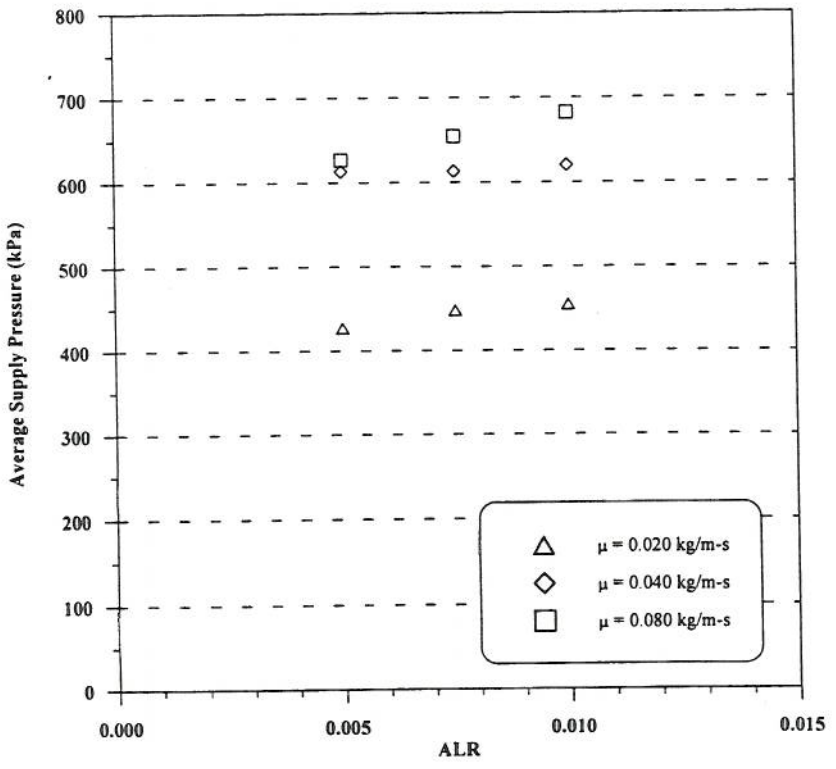

Fig. 5 Atomizer supply pressure versus air/liquid ratio (ALR) for three liquids having viscosities of 0.020, 0.040, and 0.080 kg/m-s, a common surface tension of 0.030 kg/s^2, and a common liquid mass flow rate of 0.6 g/s.

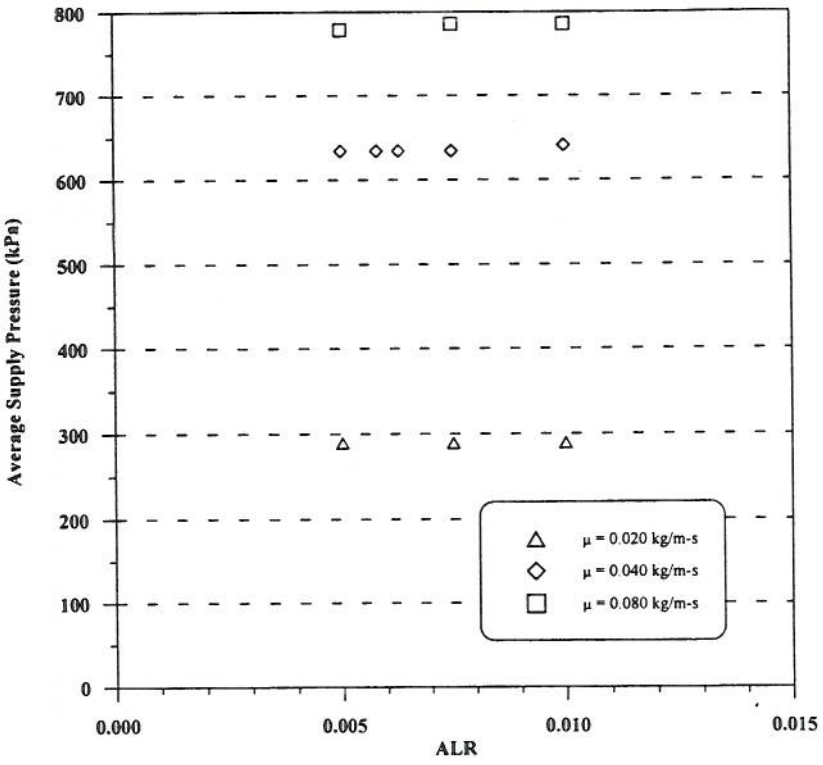

Fig. 6 Atomizer supply pressure versus air/liquid ratio (ALR) for three liquids having viscosities of 0.020, 0.040, and 0.080 kg/m-s, a common surface tension of 0.067 kg/s^2, and a common liquid mass flow rate of 0.6 g/s.

reduced as ALR goes down, and that their diameters increase. Furthermore, spray quality is observed to deteriorate markedly as ALR drops from 0.0075 to 0.005. The presence of a pronounced central liquid jet is the cause of this deterioration, since only a few large-diameter ligaments are present at this low ALR operating condition, resulting in a large value of SMD. This observation is consistent with the drop size results discussed earlier.

High-speed photography was very useful in obtaining qualitative information about how spray quality is affected by decreasing ALR. However, one limitation of the photographs presented in Figs. 8 through 12 is their inability to portray accurately the three-dimensional processes occurring at the nozzle exit plane. For that reason, focused-image holograms were obtained using the system of Santangelo and Sojka [13].

Figure 13 is an artist's rendition of the near-nozzle breakup regime as seen in various holograms. As Fig. 13 shows, the presence of the porous disk does not completely modify the two-phase flow structure, as ligaments are still preferentially formed in an annular band that surrounds a gas core. However, the porous medium does limit the diameter of ligaments formed at the nozzle exit plane for ALRs of 0.0075 and above, leading to smaller droplets. Consequently, the single bubble expansion regime that leads to the sharp rise in SMD as ALR falls below about 0.03 in the Lund et al. [9] design is delayed until ALR falls

below 0.0075 when using the design introduced here. The holographic images also support the conclusion that only a limited number of large-diameter ligaments are formed as ALR approaches 0.005.

MODEL

This section describes a model that has been developed to understand the process, and to predict which variables influence the performance, of ligament-controlled effervescent atomizers.

It was shown previously that the Lund et al. [9] model is successful in predicting mean drop size for low-mass-flow-rate effervescent atomizer-produced sprays. However, their model does have limitations. Most notably, it does not incorporate the effects of the relative velocity that exists between the two phases. The model developed during this investigation addresses this shortcoming. The geometric portion of this model is based on three-dimensional holographic images, which clearly indicate that liquid breakup proceeds through the formation of an annular band of ligaments whose individual diameters are of the order of the size of the pores in the porous medium. The analytical portion of this model

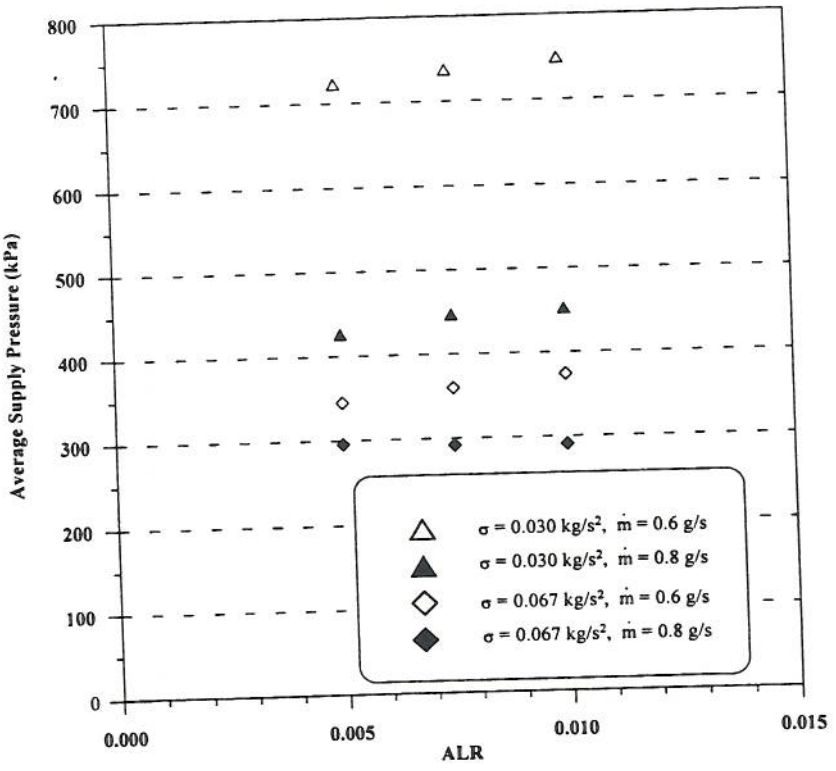

Fig. 7 Atomizer supply pressure versus air/liquid ratio (ALR) for two liquids having surface tensions of 0.030 and 0.067 kg/s², a common viscosity of 0.020 kg/m-s, and a liquid mass flow rates of 0.6 and 0.8 g/s.

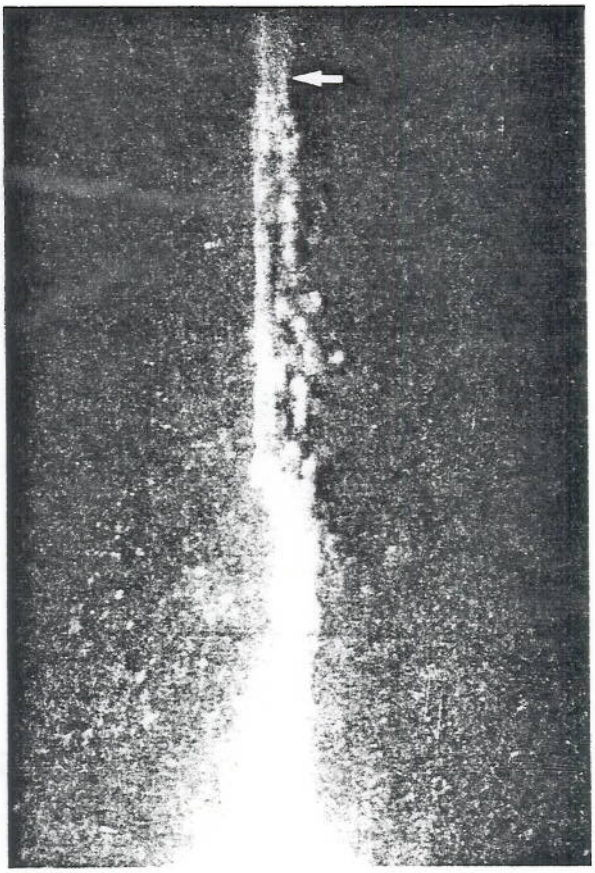

Fig. 8 Near-nozzle structure for a 1.0-g/s water spray at an ALR of 0.015 produced by a conventional effervescent atomizer (i.e., without a porous insert).

consists of determining the breakup wavelength of these ligaments. If it is further assumed that no secondary atomization takes place and that each ligament collapses into a sphere whose diameter is equal to the SMD, an expression for spray mean drop size is obtained.

The length of the ligaments was determined using the relationship developed by Sterling and Sleicher [1]. Their expression predicts the wavelength of the fastest growing disturbance in a capillary jet and accounts for the aerodynamic interaction between the jet and the surrounding medium.

$$\beta^2 + \frac{3\mu\xi^2}{\rho a^2}\beta = \frac{\sigma}{2\rho a^3}(1 - \xi^2)\xi^2 + \frac{U^2\hat{\rho}\xi^3 K_0(\xi)}{2a^2\rho K_1(\xi)} \tag{5}$$

Here β is the dimensionless growth rate of the disturbance; ξ is the dimensionless wavenumber; μ, ρ, and σ are the liquid viscosity, density, and surface tension, respectively;

$\hat{\rho}$ is the gas velocity, a is the radius of the jet, and U is the relative velocity between the liquid and gas phases.

If the jet radius and relative velocity are known, Eq. (5) can be solved numerically for the dimensionless wavenumber, ξ, that results in the largest dimensionless disturbance growth rate, β. Note that when the relative velocity between the two phases is assumed to be zero, this expression can be manipulated to obtain the Weber [10] expression for the critical wavelength.

We assume in this investigation that the ligaments can be modeled as cylindrical jets and that their diameter, d_l, is controlled by the pore size of the porous medium. Therefore, only the relative velocity between the two phases is needed to solve Eq. (5). Determining the relative velocity was the biggest challenge in modeling ligament-controlled effervescent atomizers.

Due to the difficulty in solving for the velocities of the two phases analytically as they pass through the porous medium, measured momentum rates were used to determine the

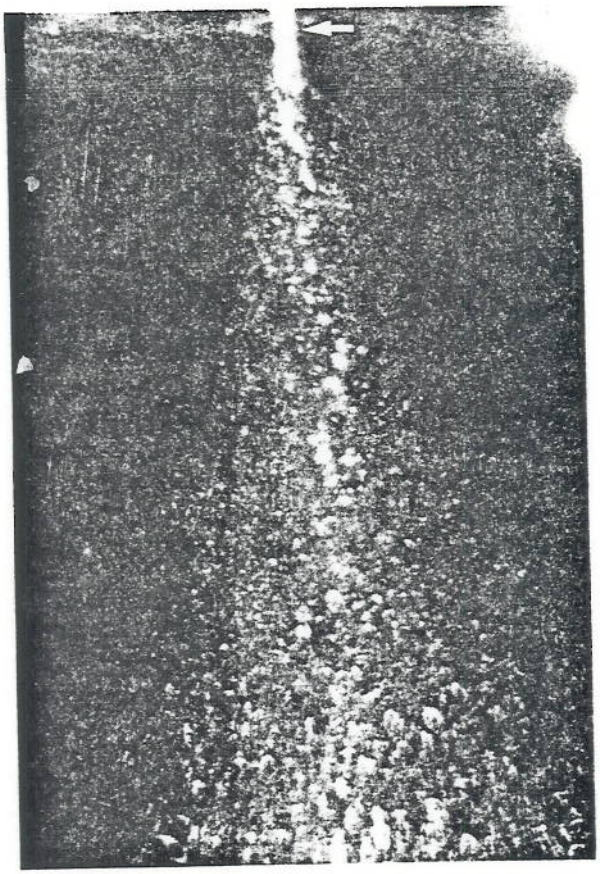

Fig. 9 Near-nozzle structure for a 1.0-g/s water spray at an ALR of 0.015 produced by a ligament-controlled effervescent atomizer (i.e., with a porous insert).

Fig. 10 Near-nozzle structure at an ALR of 0.01, mass flow rate of 0.6 g/s, viscosity of 0.020 kg/m-s, and surface tension of 0.067 kg/s^2.

liquid and gas velocities experimentally. This was accomplished using the equation derived by Deichsel and Winter [16] for determining the velocity slip ratio, sr, between the liquid and gas phases:

$$\mathrm{sr}^2 + \mathrm{sr}\left[\frac{\dot{m}_g \rho_l}{\dot{m}_l \rho_g} + \frac{\dot{m}_l}{\dot{m}_g} - \frac{A_E M_0 \rho_l}{\dot{m}_g\ \dot{m}_l}\right] + \frac{\rho_l}{\rho_g} = 0 \tag{6}$$

Here sr is the velocity slip ratio, $\dot{m}_g$ is the gas mass flow rate, $\dot{m}_l$ is the liquid mass flow rate, A_E is the area of the atomizer exit orifice, ρ_g is the gas density, ρ_l is the liquid density, and M_0 is the momentum rate at the nozzle exit. Relative velocities between the atomizing gas and liquid, as determined using Eq. (6), are presented in Table 3.

The reaction force at the nozzle (momentum rate of the spray exiting the atomizer) was measured using the apparatus of Bush et al. [17]. Their device transforms the axially flowing spray into a radial flow through use of a deflection cone that is suspended from a cantilevered beam. When the spray impacts the cone, the beam is deflected and a strain is imposed on the base of the beam. This strain is measured using precision strain gauges and appropriate signal conditioning electronics. Bush et al. [17] describe the design details of the deflection cone, strain gauge beam, and signal conditioner.

With the velocities of both the liquid and gas phases known, Eq. (5) is solved numerically for the dimensionless critical wavenumber, ξ_{opt}, that results in the fastest-growing disturbance. The critical wavenumber can then be used in a predictive equation for the mean diameter of the spray:

Fig. 11 Near-nozzle structure at an ALR of 0.0075, mass flow rate of 0.6 g/s, viscosity of 0.020 kg/m-s, and surface tension of 0.067 kg/s^2.

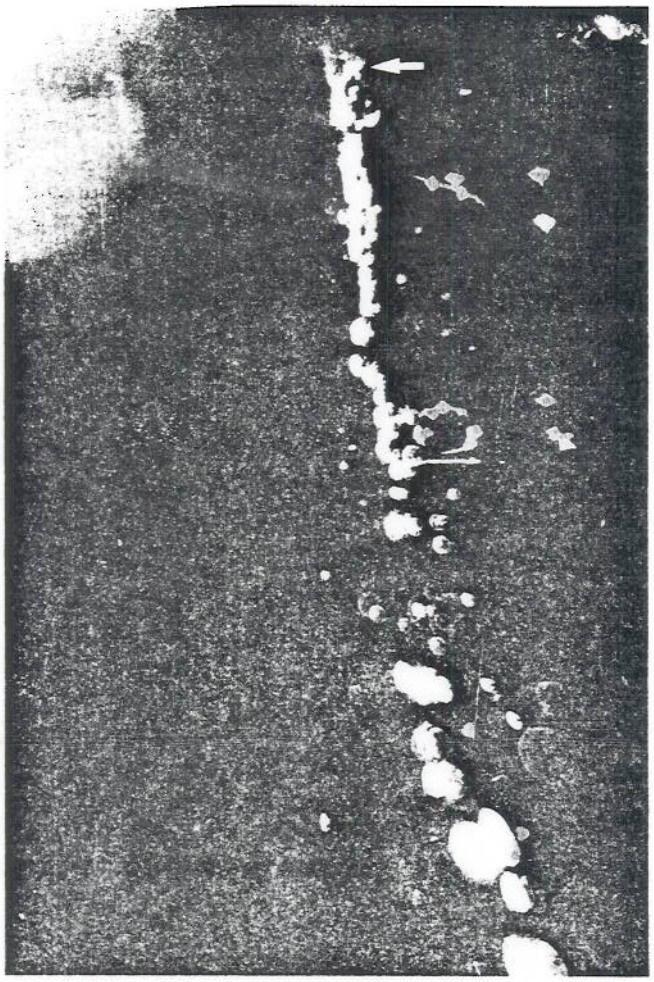

Fig. 12 Near-nozzle structure at an ALR of 0.005, mass flow rate of 0.6 g/s, viscosity of 0.020 kg/m-s, and surface tension of 0.067 kg/s^2.

$$\text{SMD} = \sqrt[3]{\frac{3\pi d_L^3}{\xi_{\text{opt}}}} \tag{7}$$

Predicted mean drop size for sprays of varying viscosities, and surface tensions of 0.030 and 0.067 kg/s^2, are plotted in Figs. 14 and 15, respectively. Experimental results are also plotted for comparison. A pore size of 37 μm was used in predicting the SMDs shown in these two figures. Spray mean drop sizes are slightly overpredicted for all cases investigated using this average pore size.

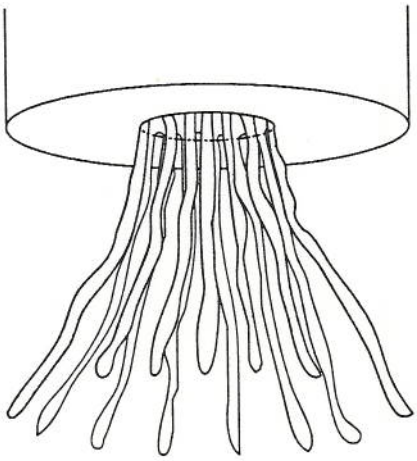

Fig. 13 Artist's rendition of a near-nozzle hologram.

Figures 16 and 17 illustrate the influence of porous-medium pore size on mean drop size by presenting predicted drop sizes assuming an average pore size of 25 μm for sprays of varying viscosities and surface tensions of 0.030 and 0.067 kg/s^2, respectively. Note that the model predictions exhibit the expected decrease in mean drop size with a decrease in porous-medium pore size (or, equivalently, ligament diameter). Also note that the mean drop size does not decrease linearly with a reduction in porous-medium pore size.

Figures 14 and 15, as well as Figs. 16 and 17, may be used to demonstrate the influence of fluid physical properties on the predicted values of the spray mean diameter. The experimental results presented in both figures indicate that the performance of ligament-controlled effervescent atomizers is relatively insensitive to the viscosity of the liquid being sprayed: Any pair of SMDs lies within the sum of their standard deviations. The predicted values of SMD obtained from the model, however, show a slight increase in mean drop size with an increase in viscosity. From a physical standpoint, viscosity dampens instabilities, leading to longer breakup lengths at higher viscosity. This leads to a larger spray mean drop size, as predicted by the model. However, the increase predicted by the model is slight, and it can therefore be concluded that the model correctly predicts the performance of ligament-controlled effervescent atomizers to be relatively insensitive to the viscosity of the fluid being sprayed.

The effects of surface tension on the predicted mean drop size of the spray can be determined by comparison of Fig. 14 with Fig. 15 (or Fig. 16 with Fig. 17). Experimental

Table 3 Relative Velocities Between Atomizing Gas and Liquid for Five Fluids at Four ALRs

Fluid	ALR = 0.0075	ALR = 0.010	ALR = 0.015	ALR = 0.020
0.020 kg/m-s, 0.030 kg/s^2	32 m/s	43 m/s	66 m/s	88 m/s
0.040 kg/m-s, 0.030 kg/s^2	36 m/s	47 m/s	72 m/s	96 m/s
0.080 kg/m-s, 0.030 kg/s^2	15 m/s	23 m/s	42 m/s	56 m/s
0.020 kg/m-s, 0.067 kg/s^2	30 m/s	42 m/s	66 m/s	90 m/s
0.040 kg/m-s, 0.0670 kg/s^2	38 m/s	49 m/s	70 m/s	93 m/s

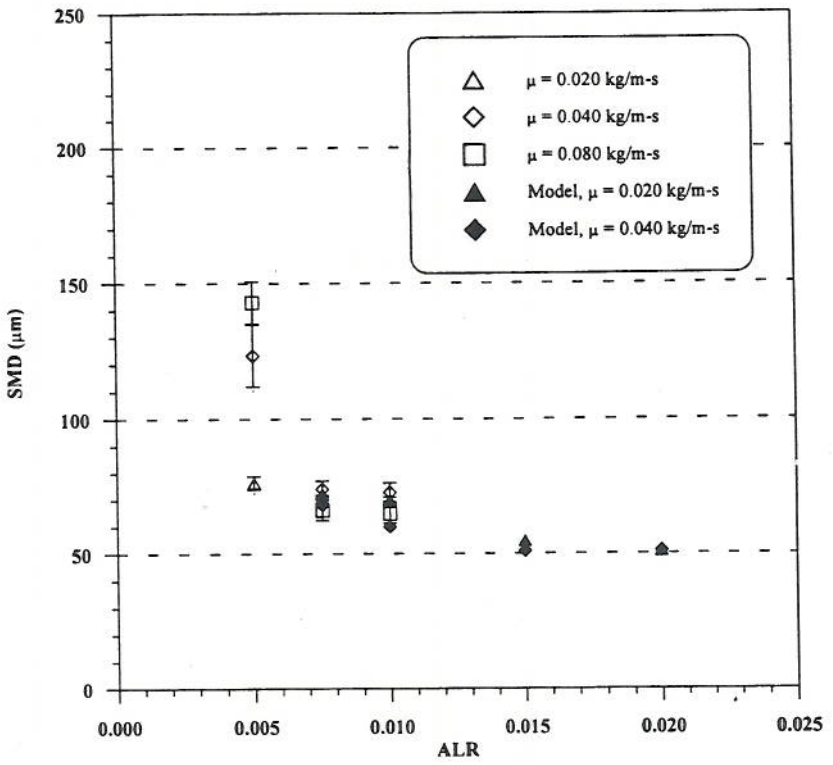

Fig. 14 Experimental data and predicted mean drop sizes, based on an average pore diameter of 37 μm, for three fluids having viscosities of 0.020, 0.040, and 0.080 kg/m-s and a common surface tension of 0.030 kg/s². Error bars represent 1 standard deviation.

results show a slight increase in mean drop size upon changing from a surface tension of 0.030 to 0.067 kg/s². This is opposite to the scaling noted by Lund et al. [9]. However, predictions obtained from the model do demonstrate a slight increase in spray mean diameter with an increase in surface tension, which agrees with the experimental results.

One of the major benefits of the Lund et al. [9] style of effervescent atomizer was that switching from an alcohol-based to a water-based carrier compound resulted in a decrease in spray mean drop size. Although the ligament-controlled effervescent atomizer does not behave in the same manner, the increase in drop size due to an increase in the surface tension is less than 10%. Furthermore, acceptable mean drop sizes were obtained using the ligament-controlled effervescent atomizer notwithstanding the increase of 10%.

The operating conditions expected to affect the predicted spray mean drop size are air/liquid ratio and liquid mass flow rate. Figures 14 through 17 show the influence of ALR on the predicted mean drop size. For the two pore sizes considered, a mean drop size of approximately 70 μm is obtained for ALRs less than 0.01. The model accurately predicts the scaling for ALRs above 0.075, but not for those below. This is due to a shift in the breakup structure of the spray that is not accounted for in the model. At very low air/liquid ratios (ALR < 0.0075), a large increase in the measured Sauter mean diameter of the spray

is noted. This is due to coalescence of the ligaments. The model developed in this study does not account for ligament coalescence and thus is unable to predict the large jump in spray mean diameter that was observed at very low ALRs.

In summary, a model to predict the mean drop size of sprays considered in this investigation was developed, based on the work of Sterling and Sleicher [1], images of the near-nozzle structure, and momentum rate measurements. The model correctly predicts mean drop size. In addition, the scaling due to surface tension, viscosity, and ALR was accurately predicted.

SUMMARY AND CONCLUSIONS

The results of this study can be summarized as follows: (1) Sub-70 μm mean drop size sprays were obtained at and below the target ALR of 0.01; (2) mean drop size was observed to increase markedly at ALRs below 0.0075, but to decrease only slightly for ALRs from 0.01 to 0.02; (3) mean drop size showed only a minor (< about 10%) increase when liquid viscosity or surface tension were increased throughout the range considered during this investigation (0.001 to 0.080 kg/m-s and 0.030 to 0.072 kg/s^2, respectively).

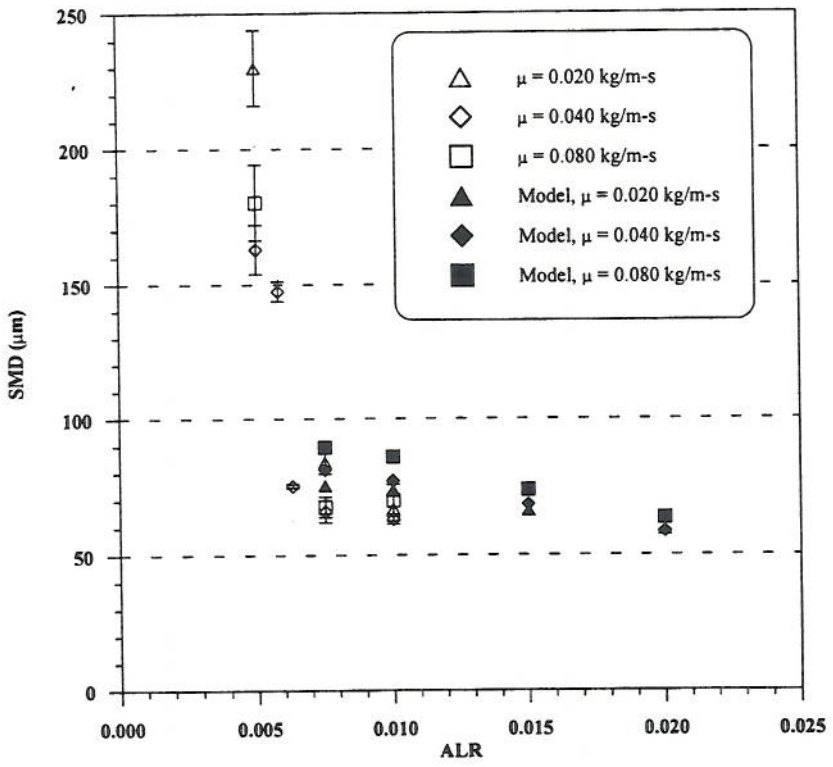

Fig. 15 Experimental data and predicted mean drop sizes, based on an average pore diameter of 37 μm, for three fluids having viscosities of 0.020, 0.040, and 0.080 kg/m-s and a common surface tension of 0.067 kg/s^2. Error bars represent 1 standard deviation.

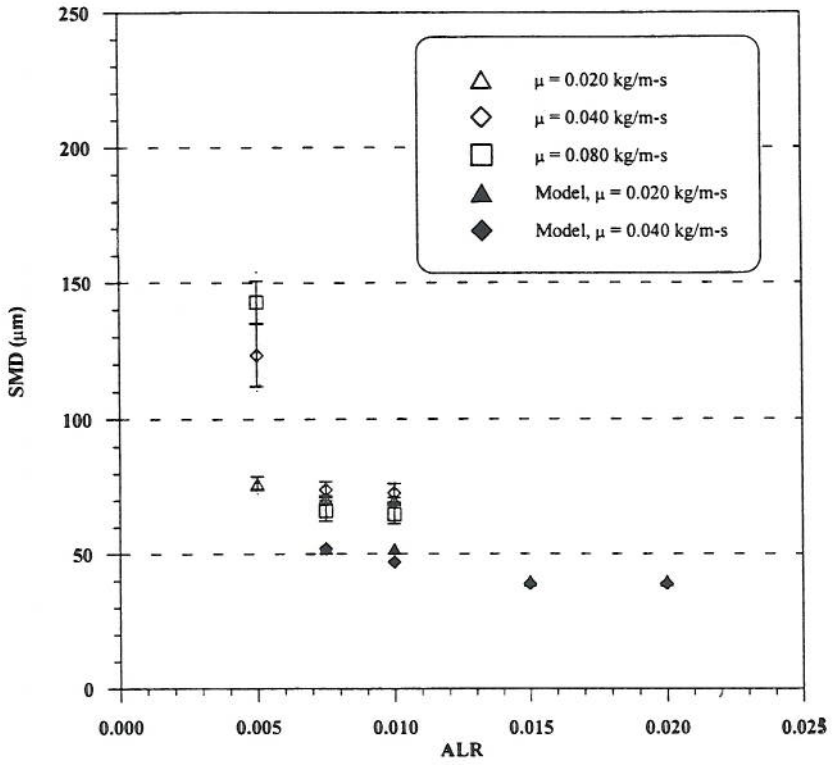

Fig. 16 Experimental data and predicted mean drop sizes, based on an average pore diameter of 25 μm, for three fluids having viscosities of 0.020, 0.040, and 0.080 kg/m-s and a common surface tension of 0.030 kg/s^2. Error bars represent 1 standard deviation.

Three-dimensional holographic and high-speed photographic images indicate why mean diameter increased markedly as ALR was reduced below 0.075: The near-nozzle breakup structure undergoes a transition from an annular band of small-diameter ligaments surrounding a gas core to a much smaller number of larger-diameter ligaments.

An analytical model was developed to describe atomizer performance. It is based on the expression of Sterling and Sleicher [1] for the instability of capillary liquid jets exposed to a moving air stream, and requires knowledge of the pore size of the porous medium and the relative velocity between the air and liquid at the nozzle exit plane. The model correctly predicts the influence of ALR, liquid surface tension, and liquid viscosity on mean drop size.

Two conclusions were drawn from the results of this study. (1) Ligament-controlled effervescent atomizers are an effective means to achieve sub-70 μm mean drop size consumer product sprays, within the supply pressure and ALR constraints imposed by DOT guidelines. They facilitate replacement of volatile organic compound solvents and hydrocarbon propellants with environmentally benign water and air. (2) The model given by Eq. (7) successfully predicts the mean drop size of ligament-controlled effervescent atomizer-produced sprays.

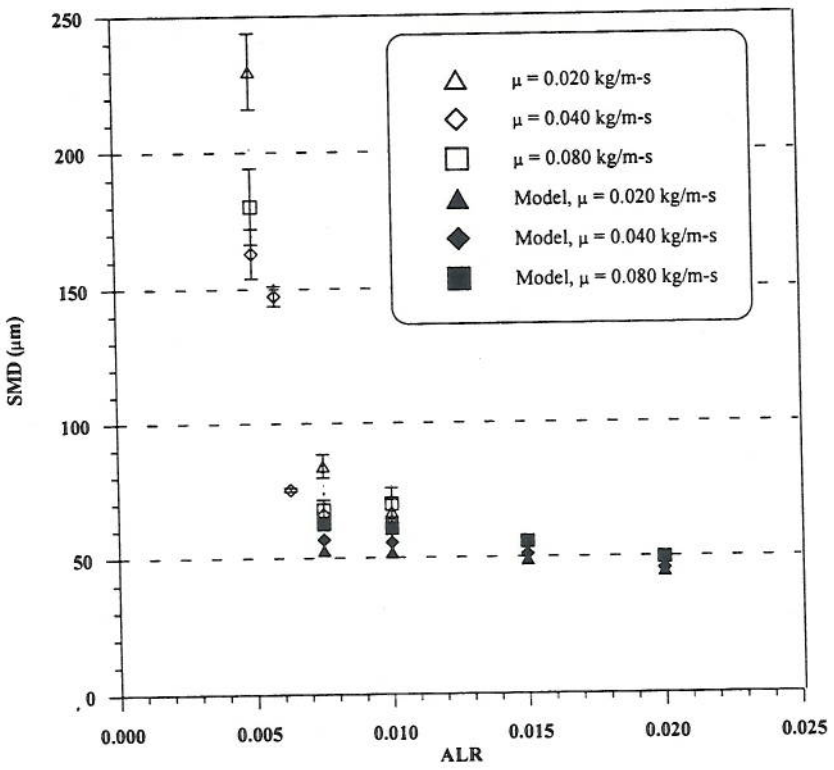

Fig. 17 Experimental data and predicted mean drop sizes, based on an average pore diameter of 25 μm, for three fluids having viscosities of 0.020, 0.040, and 0.080 kg/m-s and a common surface tension of 0.067 kg/s². Error bars represent 1 standard deviation.

REFERENCES

1. A. Sterling and C. Sleicher, The Instability of Capillary Jets, *J. Fluid Mech.*, vol. 68, no. 3, pp. 477–495, 1975.
2. A. H. Lefebvre, X. F. Wang, and C. A. Martin, Spray Characteristics of Aerated-Liquid Pressure Atomizers, *AIAA J. Propulsion Power*, vol. 4, no. 4, pp. 293–298, 1988.
3. X. F. Wang, J. S. Chin, and A. H. Lefebvre, Influence of Gas-Injector Geometry on Atomization Performance of Aerated-Liquid Nozzles, *Int. J. Turbo Jet Engines*, vol. 6, pp. 271–279, 1989.
4. T. C. Roesler and A. H. Lefebvre, Studies on Aerated-Liquid Atomization, *Int. J. Turbo Jet Engines*, vol. 6, pp. 221–229, 1989.
5. J. D. Whitlow and A. H. Lefebvre, Effervescent Atomizer Operation and Spray Characteristics, *Atomization and Sprays*, vol. 3, no. 2, pp. 137–155, 1993.
6. H. N. Buckner and P. E. Sojka, Effervescent Atomization of High Viscosity Fluids. Part II: Non-Newtonian Liquids, *Atomization and Sprays*, vol. 3, no. 2, pp. 157–170, 1993.
7. S. C. Geckler and P. E. Sojka, Effervescent Atomization of Viscoelastic Liquids, submitted.
8. P. J. Santangelo and P. E. Sojka, A Holographic Investigation of the Near-Nozzle Structure of an Effervescent Atomizer-Produced Spray, *Atomization and Sprays*, vol. 5, no. 2, pp. 137–155, 1995.

9. M. T. Lund, P. E. Sojka, A. H. Lefebvre, and P. G. Gosselin, Effervescent Atomization at Low Mass Flow Rates. Part 1: The Influence of Surface Tension, *Atomization and Sprays*, vol. 3, no. 1, pp. 77–89, 1993.
10. C. Weber, Disintegration of Liquid Jets, *Z. Angew. Math. Mech.*, vol. 11, pp. 136–159, 1931.
11. M. Ishii, One Dimensional Drift-Flux Model and Constitutive Equations for Relative Motion Between Phases in Various Two-Phase Flow Regimes, Argonne Natl. Lab. Rep. 47–77, 1977.
12. D. Reed, Porex Technologies, private communication.
13. P. J. Santangelo and P. E. Sojka, Focused-Image Holography as a Dense Spray Diagnostic, *Appl. Opt.*, vol. 33, no. 19, pp. 4132–4136, 1994.
14. P. J. Santangelo and P. E. Sojka, Holographic Particle Diagnostics, *Progr. Energy Combustion Sci.*, vol. 19, pp. 587–603, 1993.
15. P. J. Santangelo, A Holographic Investigation of the Near Nozzle Structure of an Effervescent Spray, M.S. thesis, Purdue University, West Lafayette, IN, 1993.
16. M. Deichsel and E. R. F. Winter, Adiabatic Two-Phase Pipe Flow of Air-water Mixtures Under Critical Flow Conditions, *Int. J. Multiphase Flows*, vol. 16, no. 3, pp. 391–406, 1990.
17. S. G. Bush, J. B. Bennett, P. E. Sojka, M. V. Panchagnula, and M. W. Plesniak, Momentum Rate Probe for Use with Two-Phase Flows, *Rev. Sci. Instrum.*, vol. 67, no. 5, pp. 1878–1885, 1996.